Journal of Solid State Chemistry **143,** 9–15 (1999)
Article ID jssc.1998.8052, available online at http://www.idealibrary.com on IDEAL®

Structural and Physical Properties of the Solid Solution Series $Bi_4V_{2-x}Ni_xO_{11-1.5x}$

Said Nadir and Hugo Steinfink[1]

Texas Materials Institute and Department of Chemical Engineering, University of Texas at Austin, Austin, Texas 78712

Received May 18, 1998; in revised form September 22, 1998; accepted September 24, 1998

The compounds $Bi_4V_{2-x}Ni_xO_{11-1.5x}$, $x \leq 0.35$, were prepared by solid state reaction. The α phase is present at room temperature for $x \leq 0.20$ and the γ phase is stable for greater Ni concentrations. The oxygen ion vacancies in the $x = 0.30$ phase exist in the equatorial plane of the V/Ni coordination octahedron. The $x = 0.30$ phase is paramagnetic. As the Ni concentration decreases the magnetic spin structure gradually changes to that of an amorphous spin glass. At 833 K the ionic conductivity $\sigma = 3.16 \times 10^{-2}$ S cm^{-1}. The ionic conductivity decreases with increasing Ni concentration.

INTRODUCTION

The discovery that $Bi_4V_2O_{11}$ is a good oxide ion conductor has led to intense research on this compound. It was first described by Busch *et al.* (1) and its structure is related to that of the Aurivillius phases (2). Shortly thereafter the ability of the compound to act as an oxide ion conductor was discovered by Abraham *et al.* (3). The compound evinces a complex crystal chemistry. Between room temperature and about 700°C there are three phase transitions, $\alpha \rightarrow \beta \rightarrow \gamma$, and they strongly influence the conductivity as a function of temperature. Because the high-temperature γ phase has the largest ionic conductivity numerous efforts have been devoted to stabilizing this structure at room temperature and influencing the physical properties by isomorphous replacement of the V and Bi ions (4–15a,b). The generic designation BIMEVOX has been applied to these substituted compounds. Strobel *et al.* (5) investigated the crystal structures and anion conductivity of single crystals of $Bi_4(V_{1-x}M_x)_2O_{11}$, $M =$ Cu, Ni. They report an incommensurate structure for the Cu phase but no superstructure was observed for the Ni phase. Subsequently (6) the Cu and Ni phases were investigated by powder neutron diffraction and Rietveld refinements. The atomic coordinates for one Ni substituted phase refined in space group *I*4/*mmm* yielded the composition $Bi_4V_{1.75}Ni_{0.25}O_{10.4}$. The authors state that the results were "not entirely satisfactory." For example, the Bi atom was statistically distributed over the 16*m* site of the space group to permit "a good description of the structure." Pernot *et al.* (16) report that Ni-substituted compounds with the γ structure show a very weak and complex incommensurate modulation.

We reinvestigated the properties of the solid solution series $Bi_4V_{2-x}Ni_xO_{11-1.5x}$ with particular emphasis on the crystal structure of the phase $Bi_4V_{1.7}Ni_{0.3}O_{10.4}$ determined from three-dimensional single-crystal X-ray diffraction data. We determined the magnetic susceptibility for various values of the Ni substitution as well as the ionic conductivity and report here the results.

EXPERIMENTAL

The polycrystalline specimens were prepared by solid state reaction between Bi_2O_3 (Riedel–de Haen, purity $>99\%$) and V_2O_5 (Merk, purity $>99\%$) that were preheated at 600°C and 300°C respectively, and NiO (99% as metal). The reactants were weighed in the desired stoichiometries, thoroughly ground together, and reacted in gold boats. The mixture was first heated at 700°C for 12 h followed by heating at 800°C with intermediate grinding until no further change in the powder X-ray diffraction diagrams was observed. The products were then annealed in air at 800°C and air quenched. The powder diffraction patterns were obtained with a Philips diffractometer equipped with a graphite diffracted-beam monochromator and Cu$K\alpha$ radiation. Density measurements were carried out on an automated helium gas displacement pycnometer. Two-probe impedance spectroscopy was used to measure the ac conductivity of sintered pellets. Electrical contacts were made by applying silver paint to the two ends of the pellet after it had been wet-sanded. A frequency range from 5 Hz to 13 MHz was used at an ac amplitude of 40 mV with a Hewlett–Packard 4192A IF impedance analyzer over the temperature interval $300 \leq T \leq 750$°C with an accuracy of ± 1.5°C. In the course of this study single crystals with

[1] To whom correspondence is to be addressed.

0022-4596/99 $30.00

composition $Bi_4V_{1.7}Ni_{0.3}O_{10.4}$ were prepared by melting this material and slow cooling at 2°C/h to 400°C and then cooling to room temperature at 10°C/h.

Magnetic susceptibilities were measured with a Quantum Design DC SQUID magnetometer. The specimen was introduced into the instrument and equilibrated at 6 K in zero field (ZFC). At this point a field of 1 kOe was applied and the magnetization was measured as a function of temperature to 300 K. After 1 h at 300 K, with the field remaining switched on at all times, magnetization measurements were obtained while cooling to 6 K (FC). Successive susceptibility measurements occur automatically after the temperature stabilizes.

X-RAY DIFFRACTION

A single crystal was selected and mounted on a Weissenberg camera. Oscillation and *h*0*l* diffraction photographs showed sharp spots and no evidence of an incommensurate periodicity was seen. The crystal was mounted on a Siemens P4 diffractometer. The pertinent data are shown in Table 1. Unit cell parameters were obtained by a least squares fit of 20 carefully centered reflections. The structure was determined by the direct method using SHELX93 (17), which located the cations. Subsequent difference Fourier maps located the anions. Atomic scattering values were obtained from (18). The idealized crystal structure of the γ phase of $Bi_4V_2O_{11}$ is that of the Aurivilius structure in which layers of $Bi_2O_2^{2+}$ alternate with negatively charged layers of metal octahedra; see Fig. 1 (2). The single-crystal structure analysis of one of the compounds prepared here yields the stoichiometry $Bi_4V_{1.7}Ni_{0.3}O_{10.4}$. The site occupancy factors (sof) and displacement parameters had to be refined separately; otherwise the least squares calculation diverged. One set of parameters was held fixed while the others were varied and this was done until no further changes took place. The site occupancy factors for Bi, O(1), and O(3) were within 1 esd of 0.125 so that they were fixed at full occupancy. The O(2) site is about 60% occupied. The final refinement on F^2 with the parameters shown in Table 2, anisotropic displacement parameters for the cations and isotropic for the anions, yielded $R = 0.0418$, w$R = 0.105$. Table 3 shows some selected bond lengths and angles. Figure 1 shows the crystal structure with all sites occupied. The stoichiometry $Bi_4V_{1.7}Ni_{0.3}O_{10.4}$ indicates that about 0.3 V^{5+} was reduced to V^{4+}. The disordered V/Ni site is coordinated octahedrally by O(2) and O(3). The apical O(3) sites, assumed to be fully occupied, are 1.61(12) Å from the cation but the equatorial O(2) site is only 60% occupied with V/Ni–O(2) = 1.9628(1) Å. The V/Ni–O(3) = 1.61(2) Å bond

TABLE 1
Crystal Data and Structure Refinement for $Bi_4V_{1.7}Ni_{0.3}O_{10.45}$

Empirical formula	$Bi_4Ni_{0.30}O_{10.45}V_{1.70}$
Formula weight	1108.93
Temperature (K)	293(2)
Wavelength (Å)	0.71073
Crystal system	Tetragonal
Space group	*I*4/*mmm*
Unit cell dimensions	
a (Å)	3.9255(1)
c (Å)	15.444(5)
Volume (Å^3), *Z*	237.99(8), 1
Density, calculated/measured	7.737/7.901(9)
Diffractometer	Siemens P4
Scan method	ω–2θ
Absorption coefficient	75.908 mm^{-1}
F(000)	464
Crystal faces/dimensions (mm)	001/0.01; 00$\bar{1}$/0.01; 102/0.05; $\bar{1}$0$\bar{2}$/0.05; 010/0.07; 1$\bar{2}$0/0.07
Transmission factors, min max	0.02114, 0.23299
Theta range for data collection	2.64–27.49°
Limiting indices	$-5 \leq h \leq 5$, $-5 \leq k \leq 5$, $-20 \leq l \leq 20$
Standard reflections (no decay)	$\bar{1}23$, $\bar{2}\bar{1}3$. 12$\bar{3}$, 116
Reflections collected	1080
Independent reflections/R_{int}	110/0.0548
Refinement method	Full-matrix least squares on F^2
Data/restraints/parameters	110/0/11
Goodness-of-fit on F^2	1.216
Final *R* indices [$I > 2\sigma(I)$]	$R_1 = 0.0418$, w$R_2 = 0.1054$
R indices (all data)	$R_1 = 0.0418$, w$R_2 = 0.1054$
Extinction coefficient	0.018(8)
Largest diff. peak and hole (eA^{-3})	2.165 and −3.809

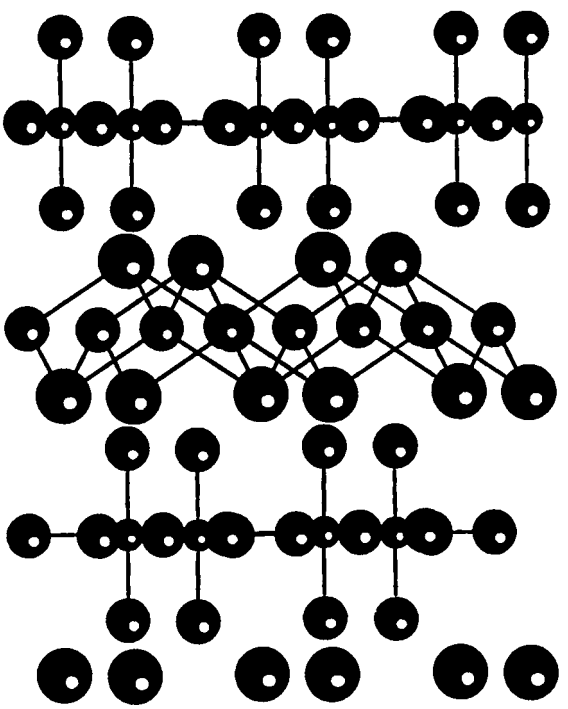

FIG. 1. The γ structure of $Bi_4V_2O_{11}$. The largest spheres are Bi, intermediate-sized spheres are O, and the small spheres are V.

TABLE 2
Atomic Coordinates, Site Occupancy Factors (Sof), and Equivalent Isotropic Displacement Parameters, (Å²)

Atom	Site	sof	x	y	z	U(eq)
Bi	4*e*	0.125	0	0	0.1693(1)	0.029(1)
V	2*b*	0.053(2)	1/2	1/2	0	0.060(5)
Ni	2*b*	0.009	1/2	1/2	0	0.060
O(1)	4*d*	0.125	0	1/2	1/4	0.022(6)
O(2)	4*c*	0.075(24)	0	1/2	0	0.11(3)
O(3)	4*e*	0.125	1/2	1/2	0.103(9)	0.22(6)

Note. U(eq) is defined as one-third of the trace of the orthogonalized U_{ij} tensor.

length is characteristic of vanadyl V^{4+} compounds but the arrangement O=V=O in an octahedron is unlikely. It is impossible to draw firm conclusions about the actual coordination polyhedron because the X-ray diffraction data provide only an average structure. The space group $I4/mmm$ constrains the atomic parameters to highly symmetric sites so that V or Ni is situated in the center of the square equatorial plane formed by O(2). It is possible that the actual configuration is that of a square pyramid as in MV_3O_7, M = Cd, Ca, Sr (19, 20). With about half of the O(2) sites vacant it is also possible that the metal ions could become tetrahedrally coordinated. The large value of U_{eq} for O(3) may be indicative of the coexistence of different coordination polyhedra in the structure.[2] The structure of a crystal with ordered oxygen vacancies and/or ordering of the substituted cations would throw a great deal of light on these conjectures.

The study of the solid solution series $Bi_4V_{2-x}Ni_xO_{11-1.5x}$ for $0.2 < x \leq 0.30$ shows that the crystal structure at room temperature is the tetragonal γ phase of $Bi_4V_2O_{11}$ over this composition range, Fig. 1. The X-ray diffraction powder patterns for the various compositions remain essentially unchanged; see Fig. 2. A very weak diffraction line can be seen at about $2\theta = 43^\circ$ that represents the strongest line of NiO. Lattice parameters for the different compositions were obtained from a least squares refinement of the indexed powder patterns and remain basically constant within 3σ, with $a = 3.934(4)$ Å, $c = 15.46(1)$ Å, for $0.225 \leq x \leq 0.30$. When $x \geq 0.35$ new, unidentified lines appear in the pattern (Fig. 2), especially the increasing intensity of the line at $2\theta \cong 27^\circ$. The solubility limit lies very close to $x = 0.30$.

In Table 4 are listed the d spacings for the X-ray diffraction powder diagram for the composition $Bi_4V_{1.7}Ni_{0.3}O_{10.4}$. For compositions with $x \leq 0.2$ the α phase of $Bi_4V_2O_{11}$ is observed.

[2] During the refereeing process a paper appeared by Abrahams *et al.* (21) reporting the defect structure of an $x = 0.2$ Ni-substituted phase determined by the Rietveldt refinement of X-ray and neutron powder diffraction data. Their conclusions essentially agree with the results reported here.

TABLE 3
Bond Lengths (Å) and Angles (°) for $Bi_4V_{1.7}Ni_{0.3}O_{10.45}$

Bi–O(1) ×4	2.3248(8)
V/Ni–O(3) ×2	1.61(12)
V/Ni–O(2) ×4	1.9628(1)
O(1)#1–Bi–O(1)#2	73.31(3)
O(1)#1–Bi–O(1)#3	115.19(6)
O(1)#2–Bi–O(1)#3	73.31(3)
O(1)#1–Bi–O(1)	73.31(3)
O(1)#2–Bi–O(1)	115.19(6)
O(1)#3–Bi–O(1)	73.31(3)

Note. Symmetry transformations used to generate equivalent atoms: #1 $x-1/2, y-1/2, -z+3/2$ #2 $x, y-1, z$, #3 $x+1/2, y-1/2, -z+3/2$ #4 $x, y, -z$, #5 $x+1, y, z$ #6 $-y+1, x, z$ #7 $-y+1, x+1, z$ #8 $x, y+1, z$ #9 $x-1/2, y+1/2, -z+3/2$, #10 $x+1/2, y+1/2, -z+3/2$, #11 $x-1, y, z$

MAGNETIC SUSCEPTIBILITY

Magnetic susceptibilities χ vs T, ZFC, of three compositions together with that of $Bi_4V_2O_{11}$ are shown in Fig. 3. As expected, the latter is diamagnetic except below about 25 K, where a paramagnetic contribution is evident. This is most likely due to the incomplete oxidation of V to the pentavalent state due to oxygen vacancies in the compound (22). The inverse susceptibility vs T for the ZFC and FC data of the $x = 0.3$ composition are identical; see Fig. 4. The data follow the Curie law and yield $\mu_{eff} = 1.2\mu_B$. The expected value for this compound, assuming noninteracting spins for Ni^{2+} ($\mu_{eff} = 3.23$) and V^{4+} ($\mu_{eff} = 1.73$), is 1.1, in good agreement with the observed value. The FC and ZFC $1/\chi$ vs T data for the phase $x = 0.25$ are shown in Fig. 5. The FC data follow the Curie law and yield $\mu_{eff} = 0.95\mu_B$. The ZFC data have a straight line section between 300 and 160 K that follow a Curie–Weiss law with $\theta \approx 50$ K. An inflection point can be detected in the curve at about that temperature and the curve thereafter turns toward the origin. The deviation from the straight line at about 160 K and the positive θ indicate that ferro- or ferrimagnetic exchange interactions are present. Below about 60 K, a straight line can be drawn for the ZFC data with $\theta \approx -11$ K, indicating that the magnetic exchange has become antiferromagnetic. The ZFC and FC curves for the $x = 0.15$ phase are shown in Fig. 6. The straight line through the three points for the ZFC data above 280 K has $\theta \approx 50$ K. Even though the data are insufficient it is noteworthy that θ remains the same. The ZFC data between 30 and 60 K can be fit with a straight line that has $\theta < 0$, while a straight line for FC data using the three points between 20 and 60 K displays $\theta > 0$. The data after the inflection point for both curves, at about 25 K, assume nearly the same values and turn toward the origin.

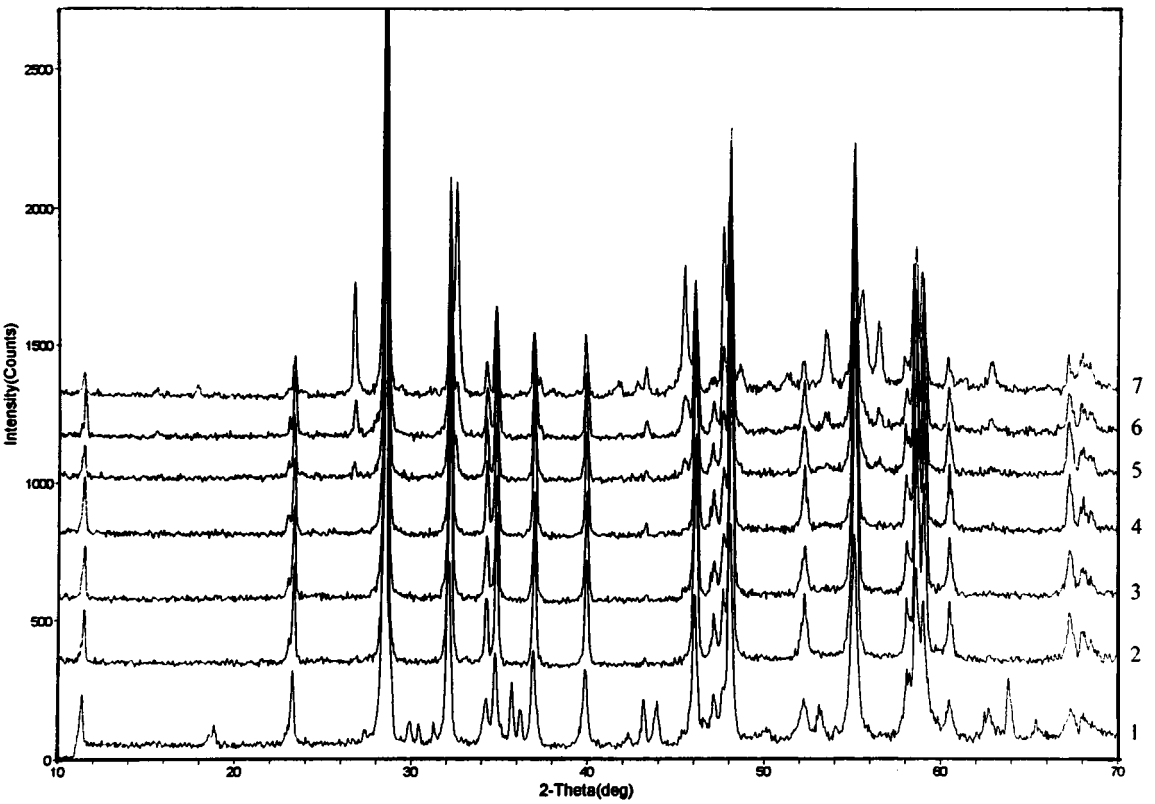

FIG. 2. The X-ray powder diffraction diagrams for $Bi_4V_{2-x}Ni_xO_{11-1.5x}$. The numbers on the right denote x values beginning with $x = 0$ (α phase), 0.225, 0.25, 0.30, 0.35, 0.40, 0.60.

With increasing dilution of the magnetic Ni^{2+} ion the magnetic behavior of the specimens gradually changes from a paramagnet to an amorphous spin structure. In such an arrangement the magnetic moments are frozen in some average local orientation but are spatially aperiodic below a freezing temperature, T_f (23). Since both the ZFC and FC $1/\chi$ data turn toward zero as T decreases it appears that the freezing temperature lies below 6 K. One would expect that below T_f the ZFC specimen would have random spins with

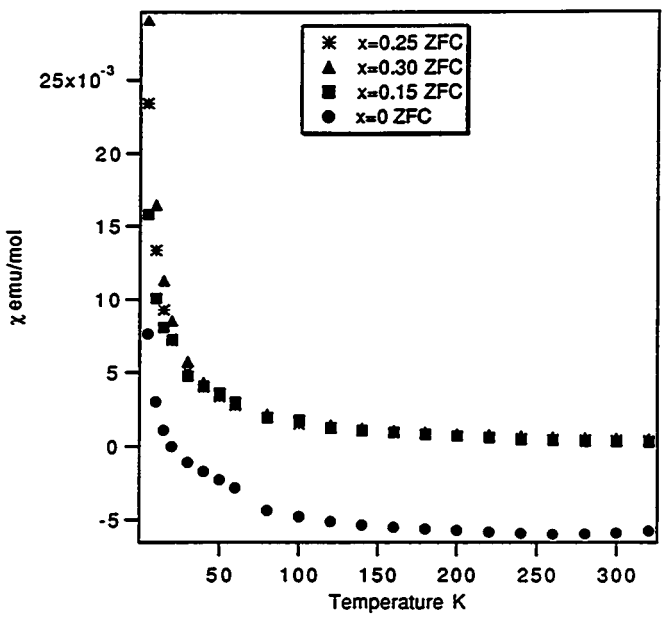

FIG. 3. The magnetic susceptibility of $Bi_4V_{2-x}Ni_xO_{11-1.5x}$.

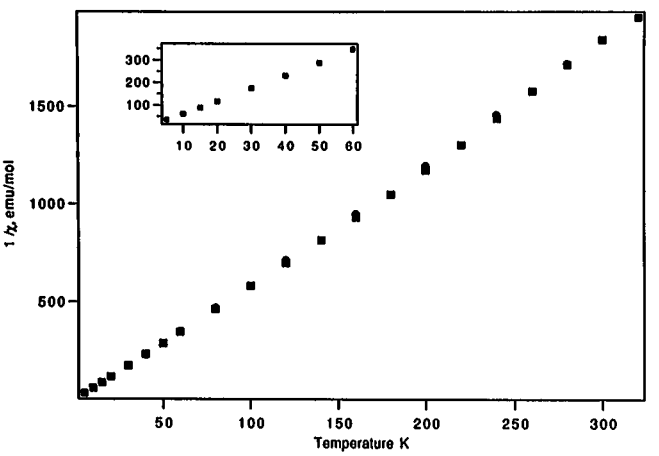

FIG. 4. The inverse magnetic susceptibility vs T for $Bi_4V_{1.7}Ni_{0.3}O_{10.45}$. (■) ZFC, (●) FC.

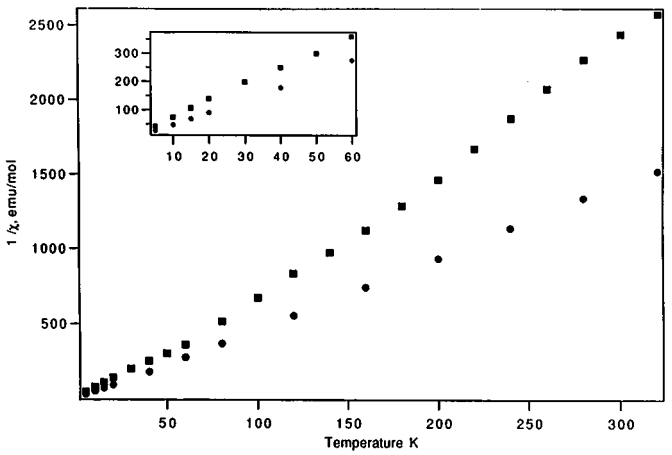

FIG. 5. The inverse magnetic susceptibility vs T for $Bi_4V_{1.75}Ni_{0.25}O_{10.625}$. (■) ZFC, (●) FC.

no net moment, a speromagnet, and that as the temperature increases past T_f the specimen would show Curie–Weiss behavior indicative of either antiferro- or ferromagnetic interactions. The data indicate that a weak ferromagnetic exchange interaction becomes dominant at higher temperatures.

ION TRANSPORT

The conductivity curves upon heating and cooling for two Ni-substituted specimens $x = 0.05, 0.10$ and of the pure V compound that have the α phase at room temperature are shown in Fig. 7. The phase transitions are visible from the changes in slope of the curves. The heating and cooling conductivity curves are reversible for the three compositions having the γ phase at room temperature and are shown in Fig. 8 for the heating cycle. The conductivity decreases with increasing Ni substitution. If it is postulated that the anion transport is the result of oxygen vacancies existing around the V/Ni octahedra, then as Ni increases on the V site and the oxygen vacancies increase, it is conceivable that the coordination polyhedron changes to a more regular configuration. This would block the mobility of the O^{2-} ions because they are now pinned to that site. To elucidate this effect it would be necessary to investigate an ordered structure. A comparison of the conductivity of the Ni $x = 0.3$ phase with other substituted compounds (11) is shown in Fig. 9. The conductivities of the Ni- and Ti-substituted phases are similar and are larger than those of the

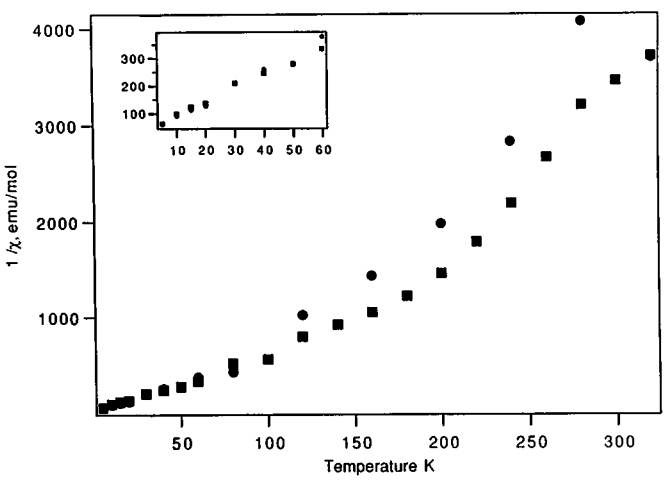

FIG. 6. The inverse magnetic susceptibility vs T for $Bi_4V_{1.85}Ni_{0.15}O_{10.775}$. (■) ZFC, (●) FC.

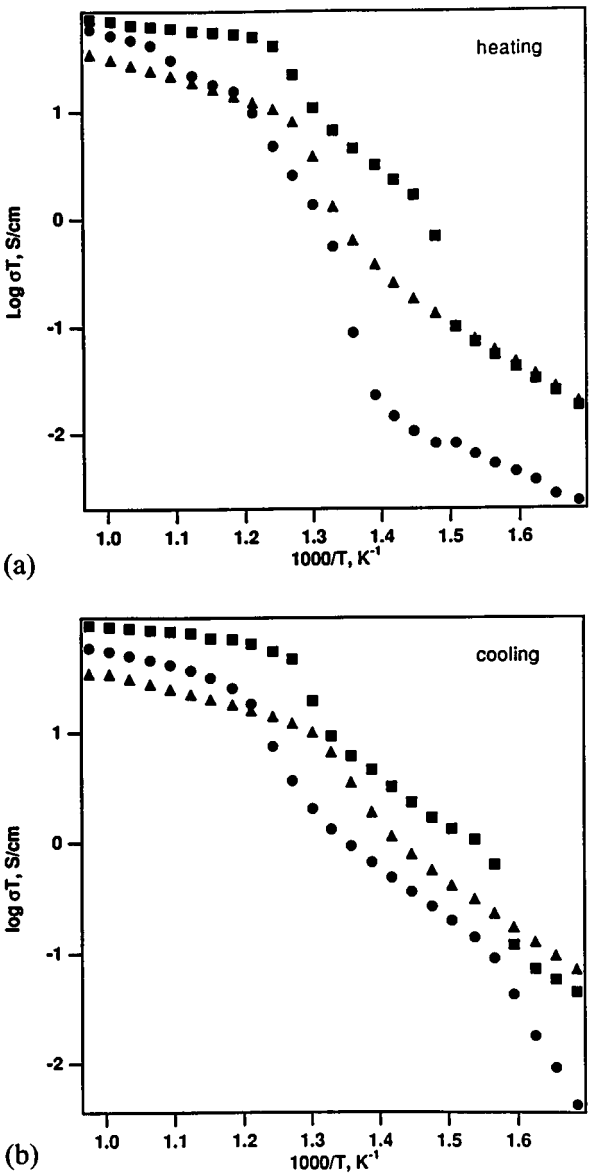

FIG. 7. Oxygen ion conductivity curves for the α phase having compositions $x = 0$ (■), 0.05 (●), and 0.1 (▲): (a) heating; (b) cooling.

TABLE 4
The Powder X-Ray Diffraction Diagram for $Bi_4V_{1.7}Ni_{0.3}O_{10.45}$

h	*k*	*l*	2θ(calc)	2θ(obs)	*d*(calc)	*d*(obs)	*I* (%)
0	0	2	11.420	11.436	7.7419	7.7314	5
0	0	4	22.990	—	3.8653	—	
1	0	1	23.294	23.339	3.8154	3.8082	8
1	0	3	28.513	28.538	3.1278	3.1252	100
1	1	0	32.137	32.158	2.7829	2.7811	36
1	1	2	34.220	34.166	2.6181	2.6222	3
0	0	6	34.804	34.763	2.5756	2.5785	14
1	0	5	36.953	36.952	2.4305	2.4306	16
1	1	4	39.898	39.902	2.2577	2.2574	12
2	0	0	46.104	46.141	1.9672	1.9657	24
0	0	8	47.015	—	1.9312	—	
1	0	7	47.178	47.143	1.9249	1.9262	3
2	0	2	47.667	—	1.9063	—	
1	1	6	48.112	48.100	1.8897	1.8901	38
2	0	4	52.140	—	1.7527	—	
2	1	1	52.292	52.298	1.7480	1.7478	8
2	1	3	55.122	55.107	1.6648	1.6652	51
1	1	8	58.107	—	1.5862	—	
1	0	9	58.636	58.633	1.5731	1.5732	32
2	0	6	59.056	—	1.5629	—	
0	0	10	59.824	—	1.5447	—	
2	1	5	60.515	60.499	1.5287	1.5290	7
2	2	0	67.271	67.250	1.3906	1.3910	7
2	0	8	67.986	68.047	1.3777	1.3766	3

Note. Space group *I*4/*mmm*, refined lattice parameters $a = 3.932(2)$ Å, $c = 15.440(8)$ Å, Cu$K\alpha_1 = 1.540562$ Å.

Cu-substituted compound. The activation energy for the Ni 0.30 composition is 0.44 eV for the straight line section of the data between 690 and 995 K. The activation energy for the straight line section of the data between 720 and 780 K is 0.49 eV for $Bi_4V_{1.7}Ti_{0.30}O_{10.85}$ (11).

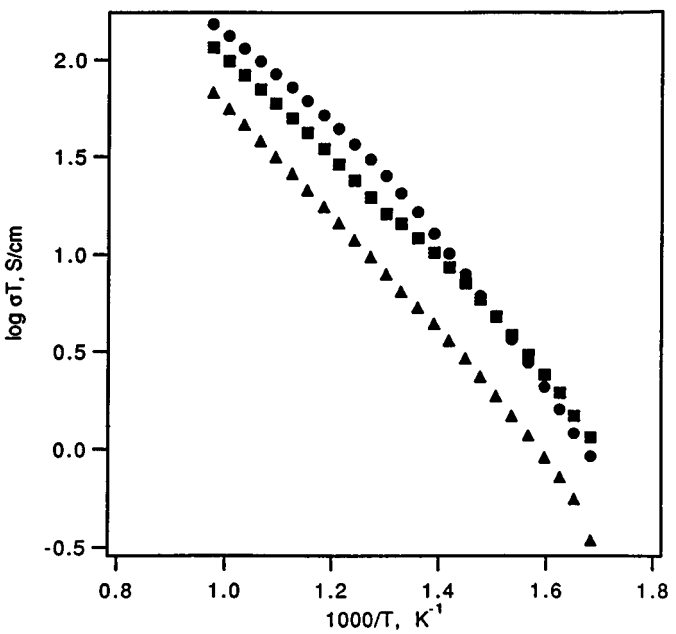

FIG. 8. The oxygen ion conductivity curves for the γ phase having compositions $x = 0.225$ (●), 0.30 (■), 0.35 (▲).

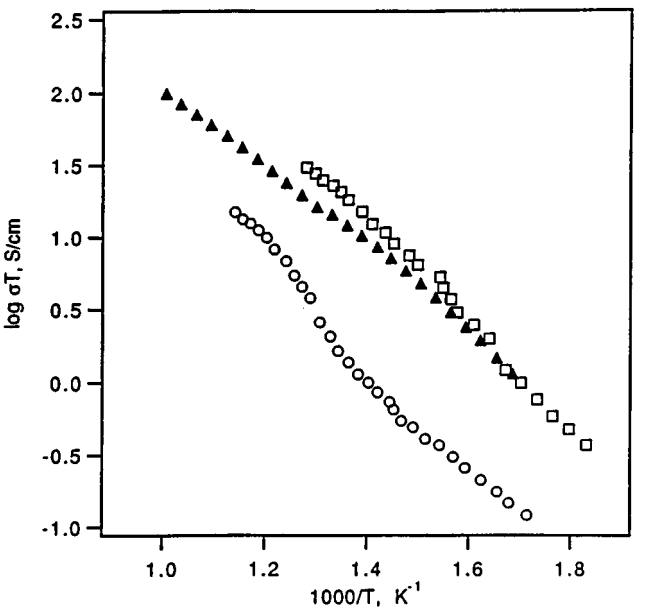

FIG. 9. The oxygen ion conductivity for $Bi_4V_{1.7}Ni_{0.3}O_{10.45}$ (▲, this study), $Bi_4V_{1.7}Ti_{0.3}O_{10.85}$ (□), and $Bi_4V_{1.8}Cu_{0.2}O_{10.7}$ (○, [11]).

CONCLUSION

The crystal structure of the phase $Bi_4V_{1.7}Ni_{0.3}O_{10.4}$ shows that Bi fully occupies the 4*e* site of space group *I*4/*mmm*, contrary to what was previously reported from a neutron diffraction analysis (6). The V and Ni ions are statistically distributed over the same crystallographic site. They occupy what would be octahedral interstices except that approximately half of the equatorial oxygen sites are vacant. It is highly likely that locally the coordination polyhedron is less symmetric. The magnetic susceptibility varies as a function of Ni substitution. The $x = 0.3$ composition is paramagnetic. As the concentration decreases to $x = 0.25$ ferro- or ferrimagnetic interactions are present. With increasing Ni dilution the material becomes an amorphous spin glass. Ion transport measurements show that the conductivity decreases with increasing Ni content. In general the values of the conductivities are comparable to those previously reported for substituted BIMEVOX.

ACKNOWLEDGMENT

The authors gratefully acknowledge the support of the Robert A. Welch Foundation, Houston, Texas.

REFERENCES

1. A. A. Bush and Yu. N. Venevtsev, *Russ. J. Inorg. Chem.* **31,** 769, (1986).
2. B. Aurivillius, *Ark. Kem.* **1,** 463 (1949).

3. F. Abraham, M. F. Debreuille-Gresse, G. Mairesse, and G. Nowogrocki, *Solid State Ionics* **28–30,** 529 (1988).
4. F. Abraham, J. C. Boivin, G. Mairesse, and G. Nowogrocki, *Solid State Ionics* **40/41,** 934 (1990).
5. P. Strobel, E. Pernot, M. Anne, M. Bacmann, J. Fouletier, T. Iharada, G. Mairesse, and F. Abraham, *in* "Proceedings of Symposium A2 on Solid State Ionics, International Conference on Advanced Materials, Strasbourg, France, 1991" (M. Balkanski, T. Takahashi, and H. L. Tuller, Eds.), Elsevier, Amsterdam/New York, 1992.
6. M. Anne, M. Bacmann, E. Pernot, F. Abraham, G. Mairesse, and P. Strobel, *Physica B* **180/181,** 621 (1992).
7. R. N. Vannier, G. Mairesse, G. Nowogrocki, F. Abraham, and J. C. Boivin, *Solid State Ionics* **53–56,** 713 (1992).
8. J. B. Goodenough, A. Manthiram, P. Paranthaman, and Y. S. Zhen, *Solid State Ionics* **52,** 105 (1992).
9. O. Joubert, A. Jouanneaux, M. Ganne, R. N. Vannier, and G. Mairesse, *Solid State Ionics* **73,** 309 (1994).
10. F. Krok, W. Bogusz, J. R. Dygas, and D. Bangobango, *Solid State Ionics* **70/71,** 211 (1994).
11. J. Yan and M. Greenblatt, *Solid State Ionics* **81,** 225 (1995).
12. R. N. Vannier, G. Mairesse, F. Abraham, and G. Nowogrocki, *Solid State Ionics* **80,** 11 (1995).
13. F. Krok, I. Abrahams, D. G. Bangobango, W. Bogusz, and J. A. G. Nelstrop, *Solid State Ionics* **86–88,** 261 (1996).
14. O. Thery, R. N. Vannier, C. Dion, and F. Abraham, *Solid State Ionics* **90,** 105 (1996).
15. (a) L. Qiu, Y. L. Yang, and A. J. Jacobson, *J. Mater. Chem.* **7,** 249 (1997). (b) Y. L. Yang, L. Qiu, and A. J. Jacobson, *J. Mater. Chem.* **7,** 937 (1997).
16. E. Pernot, M. Anne, M. Bacmann, P. Strobel, J. Fouletier, R. N. Vannier, G. Mairesse, F. Abraham, and G. Nowogrocki, *Solid State Ionics* **70/71,** 259 (1994).
17. G. Sheldrick, SHELX93, program for the refinement of crystal structures. University of Göttingen, Germany.
18. The International Union of Crystallography, "International Tables for Crystallography, Vol. C," Kluwer Academic, Dordrecht 1992.
19. J.-C. Bouloux and J. Galy, *Acta Crystallogr. Sect. B* **29,** 269 (1973).
20. G. Liu and J. E. Greedan, *J. Solid State Chem.* **103,** 139 (1993).
21. I. Abrahams, J. A. G. Nelstrop, F. Krok, and W. Bogusz, *Solid State Ionics* **110,** 95 (1998).
22. I. Abrahams, A. J. Bush, F. Krok, G. E. Hawkes, K. D. Sales, P. Thornton, and W. Bogusz, *J. Mater. Chem.* **5,** 1213 (1998).
23. K. Moorjani and J. M. D. Coey, "Magnetic Glasses," Elsevier, Amsterdam/New York, 1984.